

DiffVC-OSD: ONE-STEP DIFFUSION-BASED PERCEPTUAL NEURAL VIDEO COMPRESSION FRAMEWORK

Wenzhuo Ma and Zhenzhong Chen^{*}

School of Remote Sensing and Information Engineering, Wuhan University

ABSTRACT

In this work, we first propose DiffVC-OSD, a One-Step Diffusion-based Perceptual Neural Video Compression framework. Unlike conventional multi-step diffusion-based methods, DiffVC-OSD feeds the reconstructed latent representation directly into a One-Step Diffusion Model, enhancing perceptual quality through a single diffusion step guided by both temporal context and the latent itself. To better leverage temporal dependencies, we design a Temporal Context Adapter that encodes conditional inputs into multi-level features, offering more fine-grained guidance for the Denoising Unet. Additionally, we employ an End-to-End Finetuning strategy to improve overall compression performance. Extensive experiments demonstrate that DiffVC-OSD achieves state-of-the-art perceptual compression performance, offers about 20 \times faster decoding and a 86.92% bitrate reduction compared to the corresponding multi-step diffusion-based variant.

1 INTRODUCTION

Neural Video Compression (NVC) has progressed rapidly, surpassing traditional codecs in pixel-level distortion metrics. However, due to the inherent trade-off among rate, distortion, and perception [1], distortion-focused methods often yield suboptimal perceptual quality. This has led to growing interest in perceptual NVC, which emphasizes the rate-perception trade-off to produce clearer, more detailed, and realistic reconstructions. While GAN-based methods enhance detail through adversarial training, they remain limited by unstable training dynamics. Recently, diffusion models pre-trained on large-scale image-text datasets have emerged as a promising paradigm for perceptual NVC.

Existing diffusion-based NVCs typically adopt multi-step diffusion models, which reconstruct high perceptual quality results through multiple denoising steps. Liu et al. [2] proposed I²VC, a unified multi-step diffusion-based NVC framework supporting detail-rich reconstructions under AI, LD, and RA modes. Ma et al. [3] introduced DiffVC, which integrates a foundational diffusion model into the conditional coding paradigm using context from previously decoded frames to guide high-quality reconstruction. Although the above multi-step diffusion-based NVCs have demonstrated remarkable potential in perceptual quality, they still suffer from three major limitations. First, multi-step diffusion models usually start denoising from pure noise or noisy latent representations, which discard important structural information embedded in the latent features—information that is crucial for the compression task. Second, due to the iterative nature of multi-step inference, these models suffer from high inference latency, especially in video compression tasks where each frame requires multiple diffusion steps. Finally, due to the heavy computational burden from gradient accumulation, multi-step diffusion-based NVCs are difficult to optimize in an end-to-end manner, which limits their overall compression performance.

However, the challenges faced by the aforementioned multi-step diffusion models can be effectively addressed by a one-step dif-

fusion model. To this end, we propose **DiffVC-OSD** (One-Step Diffusion-based Perceptual Neural Video Compression), the first framework to introduce a One-Step Diffusion Model into NVC. Specifically, instead of adding noise to the reconstructed latent representation, we directly feed it into the diffusion model. By leveraging the structural information preserved in the latent and the powerful generative capacity of the diffusion model, high perceptual quality reconstructions can be achieved in just a single diffusion step. Furthermore, to more effectively integrate the one-step diffusion model into the conditional coding paradigm, we introduce a Temporal Context Adapter (TCA), which encodes the temporal context extracted from the previously decoded frame and the reconstructed latent representation into multi-level features to guide the Denoising Unet in a fine-grained manner. Finally, we employ an End-to-End Finetuning strategy that jointly optimizes the one-step diffusion model and other modules for the rate-distortion-perception trade-off, enabling optimal compression performance. Extensive experiments demonstrate that DiffVC-OSD achieves state-of-the-art perceptual compression performance across all test sets, while providing a 86.92% bitrate reduction and 20 \times faster decoding compared to its multi-step diffusion-based counterpart.

2 METHODOLOGY

As illustrated in Figure 1, we propose a One-Step Diffusion-based Perceptual Neural Video Compression framework, termed DiffVC-OSD. Built upon DiffVC [3], DiffVC-OSD follows the conditional coding paradigm and leverages Stable Diffusion V2.1-base [4] as its foundational diffusion model. The overall pipeline of DiffVC-OSD is as follows: the Motion Modules (highlighted in green) first estimate and encode the motion vector v_t between the current frame x_t and the previously decoded frame \hat{x}_{t-1} . Next, x_t is encoded into a latent representation y_t using the encoder of Stable Diffusion. The Contextual Modules (highlighted in orange) utilize the feature F_{t-1} of the previously decoded frame along with the reconstructed motion vector \hat{v}_t to perform motion compensation, and extract multi-level temporal contexts (C_t^0 and C_t^1) to support the encoding and decoding of y_t . The One-Step Diffusion Model (highlighted in red) takes the noise-free reconstructed latent representation \bar{y}_t as input

^{*}Corresponding author: Zhenzhong Chen, E-mail:zzchen@ieee.org

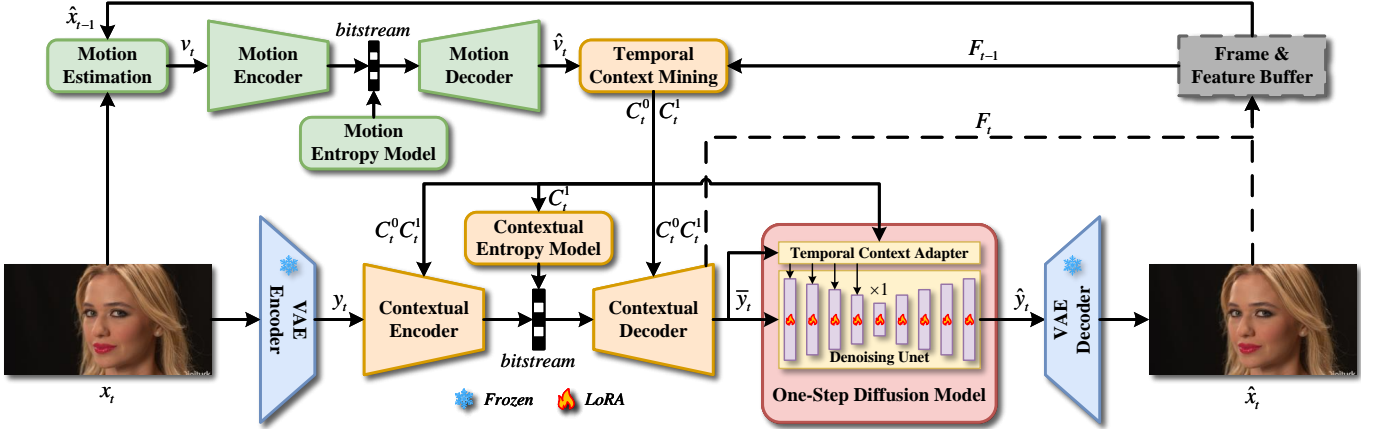


Figure 1: The framework of DiffVC-OSD.

and refines it in a single diffusion step, using both the large-scale temporal context C_t^0 and \bar{y}_t itself as conditions to enhance perceptual quality. Finally, the enhanced latent \hat{y}_t is decoded by the Stable Diffusion decoder to produce the reconstructed frame \hat{x}_t with rich details and a realistic appearance. In the following sections, we present detailed descriptions of the proposed One-Step Diffusion Model, Temporal Context Adapter, and End-to-End Finetuning strategy.

2.1 One-Step Diffusion Model

In multi-step diffusion-based NVC, the reconstructed latent representation \bar{y}_t is typically perturbed by Gaussian noise until it approximates pure noise, and then a denoising process is performed through multiple diffusion steps (e.g., 50 steps) to obtain the enhanced latent \hat{y}_t . However, the noisy latent loses important structural information that is crucial for compression task, and the need for multiple diffusion steps per video frame leads to significant inference latency, severely limiting the potential of multi-step diffusion-based NVC.

To address these issues, we introduce the One-Step Diffusion Model. Specifically, instead of adding noise, we directly feed \bar{y}_t into the Denoising Unet, thereby preserving the structural information embedded in \bar{y}_t and providing a more informative starting point for the diffusion process. Considering the temporal dependencies in video and the 'ready-made' temporal context in conditional coding paradigms, we concatenate \bar{y}_t with large-scale temporal context C_t^0 as conditions c_t to guide the diffusion model to generate a perceptually enhanced \hat{y}_t . Following the DDPM [5], the one-step diffusion process can be described as:

$$\begin{aligned} \epsilon_\theta &= \text{Unet}(\bar{y}_t, c_t, n), \text{ where } c_t = \text{Concat}(\bar{y}_t, C_t^0) \\ \hat{y}_t &= \frac{1}{\sqrt{\alpha^n}}(\bar{y}_t - \frac{1 - \alpha^n}{\sqrt{1 - \bar{\alpha}^n}}\epsilon_\theta) \end{aligned} \quad (1)$$

where ϵ_θ , n and $\alpha^n/\bar{\alpha}^n$ denote the noise predicted by the Denoising Unet, the input timestep to the Unet, and the noise scheduler coefficient of the forward diffusion process at timestep n , respectively. Leveraging the powerful generative prior of the foundational diffusion model, the One-Step Diffusion Model is capable of significantly enhancing perceptual quality with only a single diffusion step.

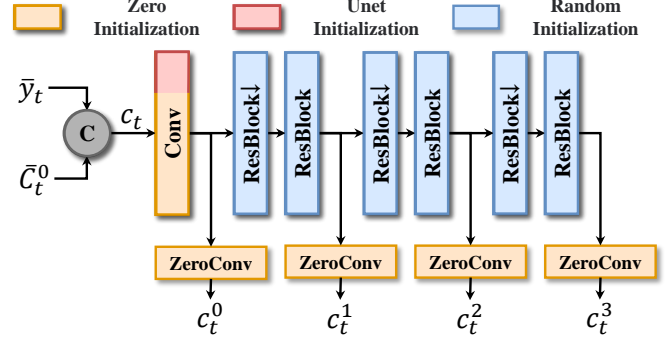


Figure 2: The structure of TCA.

2.2 Temporal Context Adapter

To enable the Denoising Unet to better leverage the condition c_t by incorporating temporal context from the previously decoded frame—rather than relying solely on the current frame—we propose the Temporal Context Adapter (TCA), as illustrated in Figure 2. Specifically, TCA takes the concatenation of \bar{y}_t and \bar{C}_t^0 as input and extracts multi-level features through convolutional layers and ResBlocks. Inspired by ControlNet [6], we adopt a special initialization strategy for the first convolutional layer of TCA: the first $N_{\bar{y}_t}$ channels are initialized with the weights from the first convolutional layer of the Unet, while the remaining $N_{\bar{C}_t^0}$ channels are initialized to zero. Here, $N_{\bar{y}_t}$ and $N_{\bar{C}_t^0}$ denote the number of channels in \bar{y}_t and \bar{C}_t^0 , respectively. Furthermore, each intermediate feature produced by TCA is passed through a zero-initialized convolutional layer to generate the final multi-level features $\{c_t^0, c_t^1, c_t^2, c_t^3\}$. These special designs allows TCA to gradually and stably learn to extract useful features, thereby facilitating the Unet in generating \hat{y}_t with high perceptual quality.

2.3 End-to-End Finetuning Strategy

DiffVC-OSD adopts a nine-stage training strategy to fully optimize each component of the model. The first seven stages follow the same procedures as those used in DiffVC [3]. In stage eight, to adapt the Denoising Unet to the video compression task, we apply LoRA [16] for lightweight fine-tuning, while freezing all other modules except for the TCA and the LoRA parameters.

Table 1: BD-rate \downarrow (%) / BD-metric \uparrow for different methods on HEVC, MCL-JCV and UVG dataset. The anchor is VTM-17.0.

Dataset	Method	Perception				Distortion	
		DISTS	LPIPS	KID	FID	PSNR	MS-SSIM
HEVC	HM-16.25 [7]	0.7 / -0.0002	17.6 / -0.0088	-17.0 / 0.0056	-11.0 / 2.9019	37.8 / -0.9235	33.0 / -0.0057
	VTM-17.0 [8]	0.0 / 0.0000	0.0 / 0.0000	0.0 / 0.0000	0.0 / 0.0000	0.0 / 0.0000	0.0 / 0.0000
	DCVC-TCM [9]	105.8 / -0.0249	53.1 / -0.0201	67.9 / -0.0188	61.8 / -13.8688	38.7 / -0.9163	10.2 / -0.0015
	DCVC-HEM [10]	53.9 / -0.0140	9.2 / -0.0040	31.0 / -0.0091	26.3 / -6.3837	-0.3 / -0.0097	-15.3 / 0.0019
	DCVC-DC [11]	25.2 / -0.0073	-7.0 / 0.0029	15.4 / -0.0049	11.2 / -2.9970	-19.8 / 0.5900	-28.5 / 0.0042
	DCVC-FM [12]	21.0 / -0.0063	-7.3 / 0.0032	13.5 / -0.0045	8.3 / -2.2913	-16.4 / 0.4788	-23.3 / 0.0036
	SEVC [13]	25.7 / -0.0078	-4.9 / 0.0022	19.4 / -0.0066	14.8 / -4.0647	-25.6 / 0.8075	-32.0 / 0.0052
	DVC-P [14]	122.9 / -0.0278	195.2 / -0.0609	75.3 / -0.0167	96.7 / -18.3528	359.0 / -4.2982	241.0 / -0.0211
	PLVC [15]	-27.1 / 0.0110	-66.9 / 0.0518	-47.3 / 0.0216	-28.7 / 10.7095	262.4 / -3.7475	120.0 / -0.0209
	DiffVC [3]	-79.0 / 0.0391	-64.8 / 0.0401	-75.8 / 0.0281	-47.8 / 14.0877	N/A / -6.4813	N/A / -0.0453
MCL-JCV	DiffVC-OSD	N/A / 0.0428	-77.1 / 0.0457	N/A / 0.0285	-56.9 / 14.6704	N/A / -6.4733	657.8 / -0.0457
	HM-16.25 [7]	0.6 / -0.0001	23.7 / -0.0118	-2.6 / 0.0003	6.2 / -0.8585	40.2 / -0.7545	37.5 / -0.0049
	VTM-17.0 [8]	0.0 / 0.0000	0.0 / 0.0000	0.0 / 0.0000	0.0 / 0.0000	0.0 / 0.0000	0.0 / 0.0000
	DCVC-TCM [9]	190.5 / -0.0328	124.3 / -0.0378	125.7 / -0.0087	96.9 / -8.5371	24.9 / -0.4232	24.5 / -0.0024
	DCVC-HEM [10]	128.7 / -0.0249	79.3 / -0.0270	93.4 / -0.0069	64.9 / -6.1862	-10.9 / 0.2178	-1.3 / -0.0000
	DCVC-DC [11]	95.8 / -0.0208	56.6 / -0.0213	64.0 / -0.0053	44.9 / -4.7827	-22.3 / 0.4831	-10.4 / 0.0011
	DCVC-FM [12]	90.2 / -0.0210	58.5 / -0.0224	67.8 / -0.0061	48.4 / -5.6161	-16.1 / 0.3549	-7.0 / 0.0008
	SEVC [13]	89.6 / -0.0211	56.4 / -0.0217	62.9 / -0.0058	38.4 / -4.6186	-28.6 / 0.6769	-21.0 / 0.0026
	DVC-P [14]	160.8 / -0.0334	236.5 / -0.0753	186.6 / -0.0117	237.2 / -18.1484	465.4 / -3.8693	388.0 / -0.0214
	PLVC [15]	-67.6 / 0.0300	N/A / 0.0857	-58.3 / 0.0082	19.5 / -2.0915	384.6 / -3.9255	296.0 / -0.0247
UVG	DiffVC [3]	N/A / 0.0556	N/A / 0.0868	-52.5 / 0.0054	0.2 / -0.3386	N/A / -6.3123	509.2 / -0.0296
	DiffVC-OSD	N/A / 0.0694	N/A / 0.1015	N/A / 0.0104	-60.1 / 5.7259	1026.2 / -4.9601	444.4 / -0.0261
	HM-16.25 [7]	-16.1 / 0.0048	3.6 / -0.0014	-5.7 / 0.0005	-0.2 / -0.0011	36.0 / -0.6329	29.2 / -0.0046
	VTM-17.0 [8]	0.0 / 0.0000	0.0 / 0.0000	0.0 / 0.0000	0.0 / 0.0000	0.0 / 0.0000	0.0 / 0.0000
	DCVC-TCM [9]	165.7 / -0.0237	94.8 / -0.0300	126.9 / -0.0036	92.1 / -3.1260	22.4 / -0.3524	27.2 / -0.0032
	DCVC-HEM [10]	112.3 / -0.0178	62.1 / -0.0215	90.5 / -0.0026	55.7 / -1.9832	-14.0 / 0.2809	0.4 / -0.0002
	DCVC-DC [11]	89.4 / -0.0160	43.5 / -0.0168	85.3 / -0.0031	54.1 / -2.2883	-25.8 / 0.5460	-11.6 / 0.0015
	DCVC-FM [12]	95.1 / -0.0181	38.1 / -0.0151	65.9 / -0.0030	39.9 / -2.0906	-20.4 / 0.4366	-8.1 / 0.0011
	SEVC [13]	105.8 / -0.0194	43.4 / -0.0168	51.1 / -0.0022	38.1 / -1.8837	-30.6 / 0.6825	-16.3 / 0.0023
	DVC-P [14]	199.4 / -0.0325	226.3 / -0.0728	306.0 / -0.0080	295.8 / -9.2418	528.6 / -4.0096	434.7 / -0.0274

* Red and Blue indicate the best and the second-best performance, respectively. 'N/A' indicates that BD-rate cannot be calculated due to the lack of overlap.

The model is optimized using the following loss function:

$$L_8 = w_1 \text{MSE}(x_t, \hat{x}_t) + w_2 \text{LPIPS}(x_t, \hat{x}_t) + w_3 \text{DIST}(x_t, \hat{x}_t) \quad (2)$$

where w_1 , w_2 and w_3 are the weights for distortion or perceptual loss terms. Typically, multi-step diffusion-based NVC methods require iterative inference, which makes end-to-end training difficult due to the high computational overhead associated with gradient accumulation. In contrast, DiffVC-OSD performs only a single diffusion step, enabling efficient end-to-end finetuning without such burdens. Specifically, in stage nine, we optimize the entire DiffVC-OSD framework using a rate-distortion-perception loss defined as:

$$L_9 = R(v_t) + R(y_t) + w_t \cdot \lambda (w_4 \text{MSE}(x_t, \hat{x}_t) + w_5 \text{LPIPS}(x_t, \hat{x}_t) + w_6 \text{DIST}(x_t, \hat{x}_t)) \quad (3)$$

where $R(v_t)$ and $R(y_t)$ denote the bitrates of the motion vector v_t and the current frame's latent representation y_t , respectively. The coefficients w_4 , w_5 , and w_6 are the weights for the respective loss terms, and λ controls the trade-off between bitrate and reconstruction quality. Additionally, w_t is a periodically varying weight following DCVC-DC [11].

3 EXPERIMENTS

3.1 Experimental Setting

Training: We use the Vimeo-90k dataset [17] for training. Following the same setup as DiffVC [3], we set four λ values: {16, 48, 128, 384}. In stage eight, the weights w_1 , w_2 and w_3 are set to 10.0, 1.0 and 1.0, respectively. The batch size is set to 30, and the model is trained for 7 epochs. The initial learning rate is 3e-4 and is decayed to 1e-4, 5e-5, and 1e-5 at the 3rd, 5th, and 7th epochs, respectively. In stage nine, the weights w_4 , w_5 and w_6 are set to 0.8, 0.08 and 0.08, and the w_t for four consecutive frames are set to {0.5, 1.2, 0.5, 0.9}. The batch size is set to 10, and the model is trained for 1 epoch with a constant learning rate of 5e-6. All experiments are conducted on RTX 3090 GPUs.

Evaluation: We evaluate the proposed method on three benchmark datasets: HEVC [18], MCL-JCV [19], and UVG [20]. Following prior works [3, 11], we evaluate the first 96 frames of each video sequence, with the intra-period set to 32. The low-delay encoding configuration is adopted, and I-frames are encoded using DCVC-DC Intra [11]. To comprehensively and quantitatively evaluate compression performance, we adopt several established metrics. For perceptual metrics, we use LPIPS [21], DIST [22], KID [23] and FID [24]. For distortion metrics, we report PSNR and MS-SSIM [25]. Finally, we use Bits Per Pixel (BPP) to measure the bitrate consumption per pixel per frame.

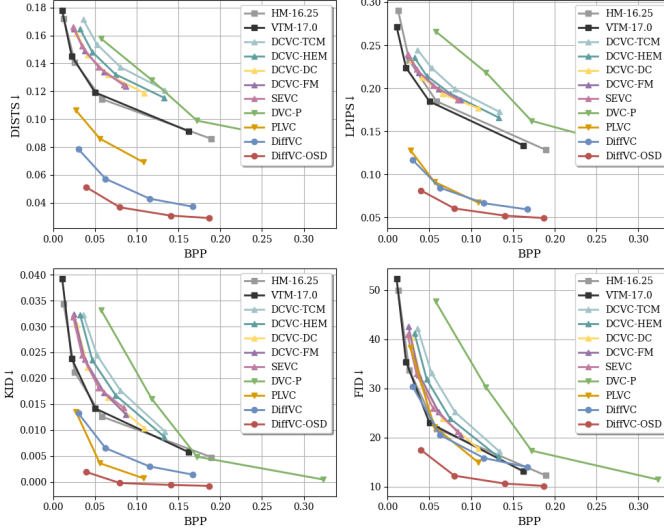


Figure 3: The rate-perception curves of the DiffVC-OSD and other video compression methods on the MCL-JCV dataset.

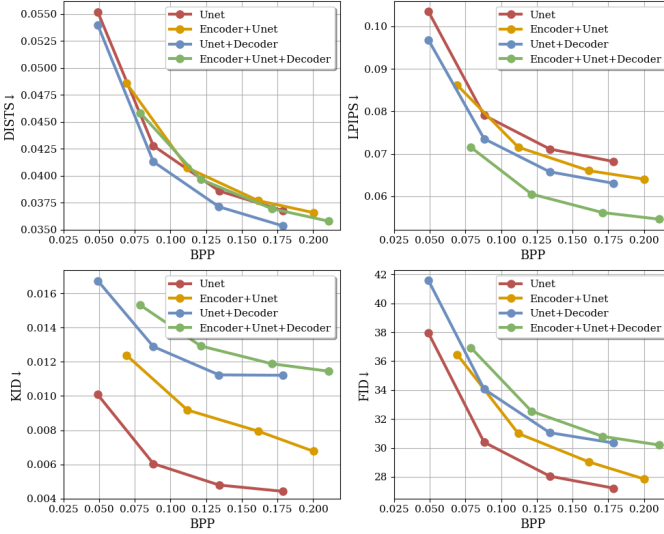


Figure 4: The ablation of lora position.

3.2 Experimental Results and Analysis

To evaluate different categories of video compression methods, we select several representative approaches from each category for comparison. Traditional codecs include HM-16.25 [7] and VTM-17.0 [8]. Distortion-oriented NVCs include DCVC-TCM [9], DCVC-HEM [10], DCVC-DC [11], DCVC-FM [12], and SEVC [13]. GAN-based NVCs include DVC-P [14] and PLVC [15], while diffusion-based NVCs include DiffVC [3] and our proposed DiffVC-OSD. Figure 3 shows the rate–perception curves of these methods on the MCL-JCV dataset. Table 1 summarizes their compression performance across three benchmark datasets, measured using BD-rate and BD-metric, with VTM-17.0 as the anchor. It is important to note that a lower BD-rate and a higher BD-metric indicate better compression performance. Experimental results demonstrate that DiffVC-OSD achieves state-of-the-art performance on all perceptual metrics across all test datasets. Even with respect to distortion metrics, DiffVC-OSD outperforms the multi-step diffusion-based method

Table 2: The ablation of DiffVC-OSD. All results are tested on HEVC Class C with DiffVC-OSD as the anchor.

Method	Modules				BD-rate (%) ↓				Dec. Time (s) ↓	
	MSD	OSD	TCA	FT	DISTS	LPIPS	KID	FID		
A	\times	\times	\times	\times	102.38	192.37	N/A	234.31	N/A	0.19
B	\times	✓	\times	\times	6.99	7.36	34.02	10.50	14.72	0.39
C	\times	✓	✓	\times	4.77	5.35	4.56	1.75	4.11	0.40
D	✓	\times	✓	\times	56.92	61.45	156.41	72.91	86.92	8.14
DiffVC-OSD	\times	✓	✓	✓	0.00	0.00	0.00	0.00	0.00	0.40

* Dec. Time refers to the time required to decode a P frame. 'N/A' indicates that BD-rate cannot be calculated due to the lack of overlap.

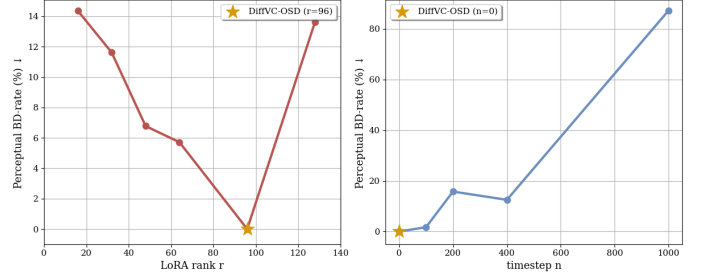


Figure 5: The ablation of LoRA rank r and timestep n .

DiffVC.

3.3 Ablation Studies

Table 2 presents the results of our ablation studies. MSD, OSD, TCA, and FT refer to the Multi-Step Diffusion Model, One-Step Diffusion Model, Temporal Context Adapter, and End-to-End Finetuning strategy, respectively. Notably, in this ablation study, MSD employs 50 diffusion steps, while all other settings remain consistent with OSD. The comparison between Method A and Method B shows that OSD achieves a significant improvement in perceptual quality by leveraging its strong generative prior, with only a 0.2s increase in decoding time. Comparing Method B and Method C, we observe that incorporating TCA yields an average improvement of 10.61% in perceptual compression performance, with a negligible decoding time increase of 0.01s. The comparison between Method C and DiffVC-OSD shows that the End-to-End Finetuning strategy results in an average 4.11% bitrate reduction on perceptual metrics. Finally, the comparison between Method C and Method D confirms that, compared to MSD, OSD provides an average 82.81% improvement in perceptual compression performance and achieves nearly 20× faster decoding speed.

Additionally, as illustrated in Figure 4, we examine the impact of inserting LoRA at different locations within the Stable Diffusion architecture. To achieve a balanced performance across four perceptual metrics, we choose to insert LoRA only into the Unet. Furthermore, Figure 5 explores how varying the LoRA rank r and timestep n fed into the Unet affects performance. Based on the results, we adopt $r = 96$ and $n = 0$ as the default configuration.

4 CONCLUSIONS

In this paper, we introduced DiffVC-OSD, a novel One-Step Diffusion-based Perceptual Neural Video Compression framework. By directly utilizing noise-free reconstructed latent repre-

sentations and applying a single-step diffusion process guided by temporal context, DiffVC-OSD achieves high perceptual quality with significantly lower decoding time. The proposed Temporal Context Adapter enhances conditional guidance, while End-to-End Finetuning further boosts overall compression efficiency. Extensive experiments demonstrate that DiffVC-OSD achieves state-of-the-art perceptual compression performance, delivering a 86.92% bitrate reduction and about 20 \times faster decoding compared to its multi-step diffusion-based counterpart. Our work highlights the potential of one-step diffusion models in advancing perceptual video compression.

REFERENCES

- [1] Yochai Blau and Tomer Michaeli. Rethinking lossy compression: The rate-distortion-perception tradeoff. In *Proceedings of the International Conference on Machine Learning*, volume 97, pages 675–685, 2019.
- [2] Meiqin Liu, Chenming Xu, Yukai Gu, Chao Yao, and Yao Zhao. I^2 vc: A unified framework for intra- & inter-frame video compression. *arXiv*, abs/2405.14336, 2024.
- [3] Wenzhuo Ma and Zhenzhong Chen. Diffusion-based perceptual neural video compression with temporal diffusion information reuse. *arXiv*, abs/2501.13528, 2025.
- [4] Robin Rombach, Andreas Blattmann, Dominik Lorenz, Patrick Esser, and Björn Ommer. High-resolution image synthesis with latent diffusion models. In *IEEE/CVF Conference on Computer Vision and Pattern Recognition*, pages 10674–10685, 2022.
- [5] Jonathan Ho, Ajay Jain, and Pieter Abbeel. Denoising diffusion probabilistic models. In *Advances in Neural Information Processing Systems*, 2020.
- [6] Lvmin Zhang, Anyi Rao, and Maneesh Agrawala. Adding conditional control to text-to-image diffusion models. In *IEEE/CVF International Conference on Computer Vision*, pages 3813–3824, 2023.
- [7] HM-16.25. <https://vcgit.hhi.fraunhofer.de/jvet/HM/>, 2022. Accessed: 2022-11-02.
- [8] VTM-17.0. https://vcgit.hhi.fraunhofer.de/jvet/VVCSoftware_VTM/, 2022. Accessed: 2022-11-02.
- [9] Xihua Sheng, Jiahao Li, Bin Li, Li Li, Dong Liu, and Yan Lu. Temporal context mining for learned video compression. *IEEE Transactions on Multimedia*, 25:7311–7322, 2023.
- [10] Jiahao Li, Bin Li, and Yan Lu. Hybrid spatial-temporal entropy modelling for neural video compression. In *ACM International Conference on Multimedia*, pages 1503–1511, 2022.
- [11] Jiahao Li, Bin Li, and Yan Lu. Neural video compression with diverse contexts. In *IEEE/CVF Conference on Computer Vision and Pattern Recognition*, pages 22616–22626, 2023.
- [12] Jiahao Li, Bin Li, and Yan Lu. Neural video compression with feature modulation. In *IEEE/CVF Conference on Computer Vision and Pattern Recognition*, pages 26099–26108, 2024.
- [13] Yifan Bian, Chuanbo Tang, Li Li, and Dong Liu. Augmented deep contexts for spatially embedded video coding. In *IEEE/CVF Conference on Computer Vision and Pattern Recognition*, pages 2094–2104, 2025.
- [14] Saiping Zhang, Marta Mrak, Luis Herranz, Marc Górriz Blanch, Shuai Wan, and Fuzheng Yang. DVC-P: deep video compression with perceptual optimizations. In *International Conference on Visual Communications and Image Processing*, pages 1–5, 2021.
- [15] Ren Yang, Radu Timofte, and Luc Van Gool. Perceptual learned video compression with recurrent conditional GAN. In *Proceedings of International Joint Conference on Artificial Intelligence*, pages 1537–1544, 2022.
- [16] Edward J. Hu, Yelong Shen, Phillip Wallis, Zeyuan Allen-Zhu, Yuanzhi Li, Shean Wang, Lu Wang, and Weizhu Chen. Lora: Low-rank adaptation of large language models. In *International Conference on Learning Representations*, 2022.
- [17] Tianfan Xue, Baian Chen, Jiajun Wu, Donglai Wei, and William T. Freeman. Video enhancement with task-oriented flow. *International Journal of Computer Vision*, 127(8):1106–1125, 2019.
- [18] Gary J. Sullivan, Jens-Rainer Ohm, Woojin Han, and Thomas Wiegand. Overview of the high efficiency video coding (HEVC) standard. *IEEE Transactions on Circuits and Systems for Video Technology*, 22(12):1649–1668, 2012.
- [19] Haiqiang Wang, Weihao Gan, Sudeng Hu, Joe Yuchieh Lin, Lina Jin, Longguang Song, Ping Wang, Ioannis Kat-savounidis, Anne Aaron, and C.-C. Jay Kuo. MCL-JCV: A jnd-based H.264/AVC video quality assessment dataset. In *IEEE International Conference on Image Processing*, pages 1509–1513, 2016.
- [20] Alexandre Mercat, Marko Viitanen, and Jarno Vanne. UVG dataset: 50/120fps 4k sequences for video codec analysis and development. In *Proceedings of the ACM Multimedia Systems Conference*, pages 297–302, 2020.
- [21] Richard Zhang, Phillip Isola, Alexei A. Efros, Eli Shechtman, and Oliver Wang. The unreasonable effectiveness of deep features as a perceptual metric. In *IEEE/CVF Conference on Computer Vision and Pattern Recognition*, pages 586–595, 2018.
- [22] Keyan Ding, Kede Ma, Shiqi Wang, and Eero P. Simoncelli. Image quality assessment: Unifying structure and texture similarity. *IEEE Transactions on Pattern Analysis and Machine Intelligence*, 44(5):2567–2581, 2022.
- [23] Mikolaj Binkowski, Danica J. Sutherland, Michael Arbel, and Arthur Gretton. Demystifying MMD gans. In *International Conference on Learning Representations*, 2018.
- [24] Martin Heusel, Hubert Ramsauer, Thomas Unterthiner, Bernhard Nessler, and Sepp Hochreiter. Gans trained by a two time-scale update rule converge to a local nash equilibrium. In *Advances in Neural Information Processing Systems*, pages 6626–6637, 2017.
- [25] Zhou Wang, Eero P Simoncelli, and Alan C Bovik. Multiscale structural similarity for image quality assessment. In *Asilomar Conference on Signals, Systems & Computers*, volume 2, pages 1398–1402, 2003.